Mitochondria-ER contact site components regulate the formation and localization of specialized high-capacity mitochondria in the *C. elegans* anchor cell.

Isabel W. Kenny-Ganzert[1], David R. Sherwood[1§]

[1]Department of Biology, Duke University, Durham, NC USA

[§]To whom correspondence should be addressed: david.sherwood@duke.edu

Abstract

Mitochondria-endoplasmic reticulum contact sites (MERCS) play crucial roles in mediating calcium signaling and lipid metabolism, and regulate mitochondrial morphology, function, and quality control. Recent studies have found that the *C. elegans* anchor cell (AC) harbors a specialized pool of high-capacity mitochondria that localize to the invasive front and are enriched with electron transport chain proteins to generate high ATP levels to fuel invasion. We conducted an RNAi screen of 59 MERCS-encoding components and identified over 30 required for high-capacity mitochondria formation. Our results suggest that MERCS may play a key role in the formation of specialized high-capacity mitochondria.

A

E

MERCS role
- Calcium
- Morphology/Dynamics
- Lipid transport
- Stress
- Tethering
- Apoptosis
- Autophagy
- ETC activity

MERCS Screen Results

C. elegans gene targeted by RNAi	Human Ortholog	MERCS Role	Abnormal ETC Enrichment	Abnormal Localization	Abnormal Morphology
L4440	Empty Vector Control	n/a	0.74%	3.10%	0%
cyn-3	PPIF		33.3% ****	0% ns	0% ns
tomm-40	TOMM40		73.3% ****	60% ****	20% **
cyn-2	PPIF		6.7% ns	26.7% ***	0% ns
djr-1.1	PARK7		0% ns	6.7% ns	6.67% ns
W08F4.3	SIGMAR1		13.3% *	0% ns	0% ns
hsp-3	BiP/HSPA5		20% **	13.3% *	0% ns
drp-1	DNM1L		80% ****	6.7% ns	0% ns
sca-1	ATP2A1		13.3% *	0% ns	0% ns
vpr-1	VAPB		6.7% ns	13.3% *	0% ns
Y54G2A.18	BCAP31		0% ns	6.7% ns	0% ns
ire-1	ERN2		6.7% ns	0% ns	0% ns
hsp-6	HSPA9		66.7% ****	33.3% ****	0% ns
sup-35	RMDN3		0% ns	13.3% *	6.7% ns
gei-1	STARD13		26.7% ***	0% ns	0% ns
ZC196.2	VAPB		0% ns	33.3% ****	33.3% ****
mff-2	MFF		46.7% ****	13.3% *	0% ns
wve-1	WASF3		33.3% ****	13.3% *	0% ns
F42G2.5	VAPB		20% **	6.7% ns	0% ns
rmd-3	RMDN3		20% **	20% **	13.3% *
hsp-4	BiP/HSPA5		33.3% ****	0% ns	0% ns
pdzd-8	PDZD8		26.7% ***	13.3% *	20% **
vdac-1	VDAC1		40% ****	0% ns	0% ns
cyn-1	PPIF		6.7% ns	26.7% ***	33.3% ****
cyn-7	PPIF		46.7% ****	0% ns	0% ns
djr-1.2	PARK7		26.7% ***	6.3% ns	6.7% ns
inft-2	INF2		20% **	13.3% *	0% ns
pacs-1	PACS2		13.3% *	6.7% ns	0% ns
fis-2	FIS1		33.3% ****	13.3% *	0% ns
atf-6	ATF6		13.3% *	20% **	6.7% ns
obr-3	OSBPL5		6.7% ns	6.7% ns	6.7% ns
pek-1	EIF2AK3		0% ns	0% ns	0% ns
rmd-1	RMDN3		53.3% ****	0% ns	0% ns
atad-3	ATAD3A		33.3% ****	33.3% ****	6.7% ns
C16C8.18	RMDN3		0% ns	0% ns	0% ns
ced-9	BCL2		13.3% *	13.3% *	6.7% ns
F36G3.3	CDIP1		20% **	6.7% ns	6.7% ns
fis-1	FIS1		6.7% ns	0% ns	0% ns
fzo-1	MFN1, MFN2		6.7% ns	0% ns	0% ns
itr-1	ITPR3		0% ns	6.7% ns	0% ns
mcu-1	MCU		33.3% ****	0% ns	20% **
rmd-2	RMDN3		13.3% *	0% ns	6.7% ns
tspo-1	TSPO		26.7% ***	13.3% *	0% ns
unc-68	RYR1		6.7% ns	0% ns	0% ns
atfs-1	ATF4		40% ****	13.3% *	6.7% ns
tdp-1	TARDBP		13.3% *	0% ns	0% ns
lrk-1	LRRK1		0% ns	0% ns	0% ns
m110.3	MARCHF5		6.7% ns	0% ns	0% ns
exc-14	MUL1		20% **	6.7% ns	0% ns
emc-1	EMC1		6.7% ns	0% ns	0% ns
fndc-1	FUNDC1		6.7% ns	0% ns	33.3% ****
hrdl-1	AMFR		6.7% ns	0% ns	20% **
miga-1	MIGA2		20% **	0% ns	13.3% *
sel-12	PSEN2		13.3% *	33.3% ****	13.3% *
T19C3.4	REEP1		0% ns	0% ns	0% ns
slc-25A46	SLC25A46		0% ns	0% ns	0% ns
mics-1	SYNJ2BP		33.3% ****	13.3% *	0% ns
tomm-70	TOMM70		46.7% ****	20% **	0% ns
T08G11.1	VPS13A		6.7% ns	6.7% ns	6.7% ns
dpy-11	TMX1		0% ns	0% ns	0% ns

15 animals scored for each gene; Empty vector control 135 animals total scored. Results from single trial, two-sided Fisher's exact test for significance, Not significant (ns), * p < 0.05, ** p < 0.01, *** p < 0.001, **** p < 0.0001

B

Mitochondria to ER Distance within 80 nm

21.553 nm
31.059 nm
24.325 nm
44.271 nm
23.474 nm

AC
VPC

C

Endoplasmic Reticulum
Mitochondria

SIGMAR1, HSPA5, ITPR3, PARK7, HSPA9, VDAC1, PPIF, TOMM Complex, PACS2, BCAP31, FIS1, DNM1L, WASF3, VAPB, ATAD3A, RMDN3, MCU, MFN1/2, PDZD8, VPS13A

D

empty vector control — NUO-1::mNG — Normal ETC Enrichment, Normal Localization, Normal Morphology

miga-1 RNAi — Abnormal ETC Enrichment, Normal Localization, Abnormal Morphology

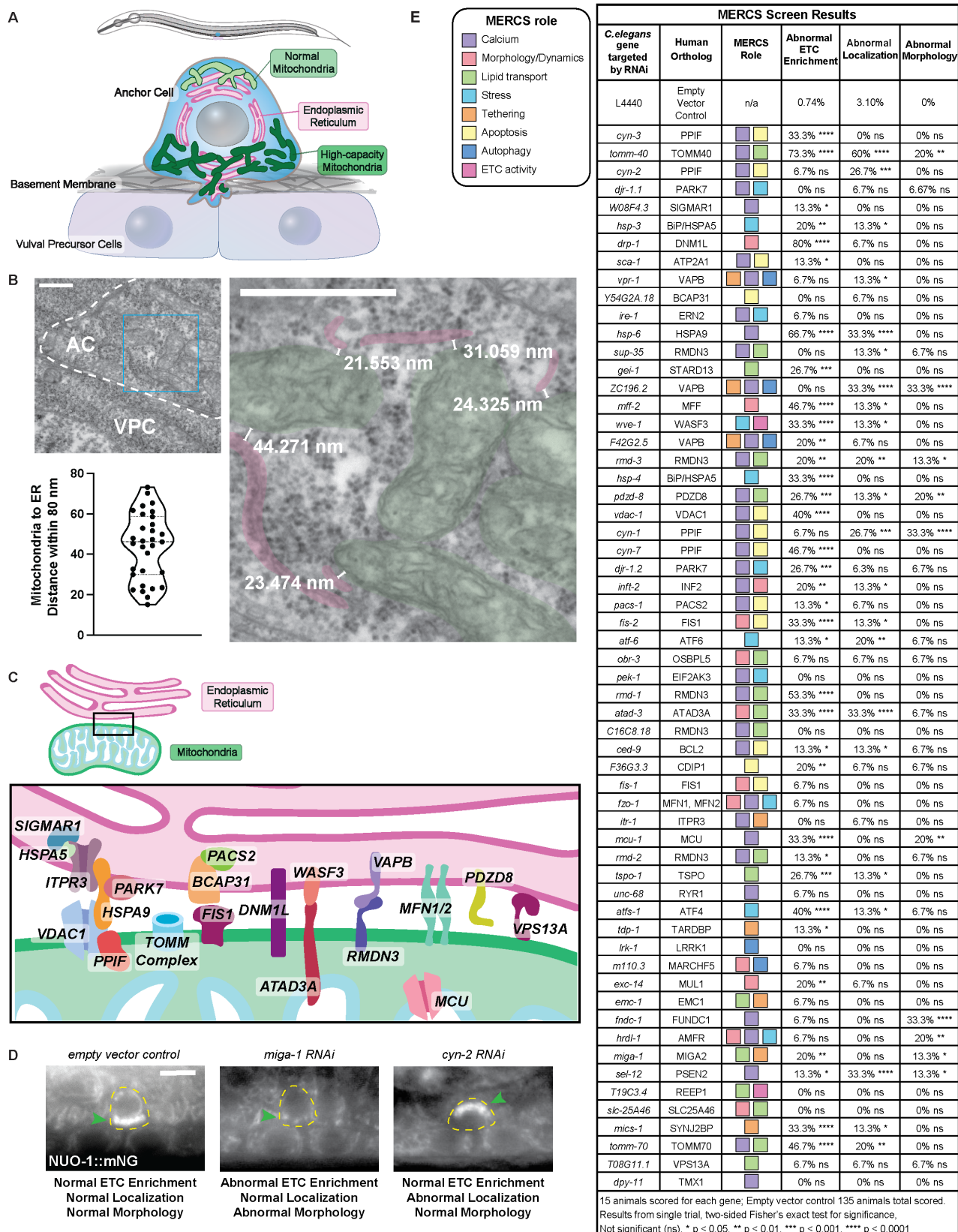*cyn-2 RNAi* — Normal ETC Enrichment, Abnormal Localization, Normal Morphology

Figure 1. Mitochondria-ER contact site components regulate high-capacity mitochondria formation and localization within the *C. elegans* anchor cell.:

A) At the L3 larval stage (top) the anchor cell (AC, blue) invades through the basement membrane (gray) to contact the vulval precursor cells (VPCs, light purple). Previous work has shown that the AC contains an extensive endoplasmic reticular (ER) network (pink) that enters the invasive protrusion (Park et al., 2024) and ETC-enriched high-capacity mitochondria that localize to the invasive front (dark green) and are a distinct population from apical lower ETC-enriched

mitochondria (light green) that are similar in composition to neighboring non-invasive cells. **(B)** (Left top) Transmission electron microscopy image of a thin section cut through the AC (dotted outline) above the VPC prior to invasion. (Right) Enlarged area of the AC corresponding to the blue box in the left panel shows where mitochondria (green) are near ER (pink). Distance (nm) measured illustrated by white bracketed line. Scale bars, 500 nm. (Bottom left) Violin plot of mitochondria to ER distance measured in mitochondria within 80 nm of ER (n = 31 mitochondria in 5 ACs). **(C)** Schematic illustration of many of the proteins with known or predicted roles in mitochondria-ER contact sites (MERCS). SIGMAR1, sigma non-opioid intracellular receptor 1 (calcium regulation); HSPA5, also known as BiP, heat shock protein family A (Hsp70) member 5 (stress); ITPR3, inositol 1,4,5-trisphosphate receptor type 3 (calcium regulation, tethering); PARK7, Parkinsonism associated deglycase (calcium regulation, stress); HSPA9, heat shock protein family A (Hsp70) member 9 (calcium regulation); VDAC1, voltage dependent anion channel 1 (calcium regulation, apoptosis); PPIF, peptidylprolyl isomerase F (calcium regulation, apoptosis); TOM Complex, translocase of outer mitochondrial membrane (calcium regulation, lipid transport); PACS2, phosphofurin acidic cluster sorting protein 2 (calcium regulation, apoptosis); BCAP31, B cell receptor associated protein 31 (apoptosis); FIS1, fission, mitochondrial 1 (morphology/dynamics, apoptosis); DNM1L, also known as DRP1, dynamin 1 like (morphology/dynamics); ATAD3A, ATPase family AAA domain containing 3A (lipid transport, ETC activity); WASF3, WASP family member 3, (stress, ETC activity); RMDN3, regulator of microtubule dynamics 3 (calcium regulation, lipid transport); VAPB, VAMP associated protein B and C (calcium regulation, tethering, autophagy); MFN1/2, mitofusin 1 and 2 (morphology/dynamics, calcium regulation, stress); PDZD8, PDZ domain containing 8 (calcium regulation, lipid transport); VPS13A, vacuolar protein sorting 13 homolog A (lipid transport). **(D)** Examples of phenotypes observed after RNAi targeting MERCS genes. (Left) Normal ETC enrichment (endogenously tagged NUO-1::mNG, arrowhead) in AC (yellow dashed line) high-capacity mitochondria localized to the invasive front treated with empty vector control RNAi. (Middle) Reduced ETC (NUO-1::mNG) enrichment, normal invasive localization, and abnormal morphology where mitochondria are more punctate and fail to form a branched network (arrowhead) after RNAi targeting *miga-1*. (Right) Normal ETC enrichment (NUO-1::mNG), normal morphology, but abnormal localization where most of the ETC-enriched mitochondria apically localized (arrowhead) after RNAi targeting *cyn-2*. Scale bar, 5 µm. **(E)** MERCS screen results.

Description

Cell invasion through basement membrane (BM) extracellular matrices (ECMs) is important in development, immune surveillance, and is dysregulated in many diseases, such as cancer (Kenny-Ganzert & Sherwood, 2024). BMs are a highly dense type of ECM. The membrane protrusions used by invasive cells to break through BMs are energetically intensive and require high ATP levels to fuel F-actin turnover, dynamic protease delivery, and active membrane trafficking (Li et al., 2019; Marshansky & Futai, 2008; Shah et al., 2015). Emerging evidence indicates that mitochondria and oxidative phosphorylation (OXPHOS) play a crucial role in delivering ATP to fuel invasive protrusions (Garde & Sherwood, 2021). An excellent model to study cell invasion through BM is the *C. elegans* anchor cell (AC). The AC is a specialized uterine cell that invades through BM during an ~90-minute window during the L3 larval stage to connect the uterine and vulval tissues to form the egg-laying apparatus (Kenny-Ganzert & Sherwood, 2024). Recent studies in our group have revealed that the *C. elegans* anchor cell (AC) relies upon specialized high-capacity mitochondria that are enriched with electron transport chain (ETC) proteins found in the folds (cristae) of the inner mitochondrial membrane (Kenny-Ganzert et al., 2025). The ETC transfers electrons through a series of protein complexes to form a proton gradient that drives ATP synthesis. These high-capacity mitochondria are concentrated at the AC's invasive front, where they provide a localized source of ATP to fuel invasion (Figure 1A) (Garde et al., 2022; Kenny-Ganzert et al., 2025). We have found that high-capacity mitochondria are specified early by the AC's pro-invasive transcriptional program, and that they require dense cristae formation and increased mitochondrial protein import machinery. We further discovered that netrin signaling through a Src family kinase directs microtubule polarization, which facilitates metaxin adaptor complex dependent high-capacity mitochondrial trafficking to the site of invasive protrusion formation (Kenny-Ganzert et al., 2025).

Mitochondria transiently connect and interact with the endoplasmic reticulum (ER) (Aoyama-Ishiwatari & Hirabayashi, 2021). The contact sites between the outer mitochondrial membrane and the ER are referred to as mitochondria–ER contact sites (MERCS). These interorganellar junctions are enriched in specific lipids and specialized proteins that define their structure and functions (Larrañaga-SanMiguel et al., 2025; Sassano et al., 2022). MERCS serve as key sites for lipid transfer and calcium (Ca^{2+}) signaling, and have functions in cellular bioenergetics, proteostasis, mitochondrial quality control, mitochondrial morphology/dynamics, apoptosis and autophagy (Flis & Daum, 2013; Giacomello & Pellegrini, 2016; Gómez-Suaga et al., 2019; Lewis et al., 2016; Loncke et al., 2021; Nakamura et al., 2025; Namba, 2019). With our recent discovery of specialized high-capacity mitochondria, we wanted to determine if MERCS might have a role in their formation and invasive enrichment.

MERCS form between juxtaposed mitochondria and ER membranes that are ~10 – 80 nm apart (Giacomello & Pellegrini, 2016; Larrañaga-SanMiguel et al., 2025). Transmission electron microscopy (TEM) can be used to identify MERCS, although the thin 2D sectioning is limited in detecting most MERCS due to their dynamic nature, as MERCS rapidly form and disassemble (Bernhard & Rouiller, 1956; Giamogante et al., 2020; Larrañaga-SanMiguel et al., 2025). Using thin

sectioned (35 – 50 nm) transmission electron microscopy images taken from five ACs (Hall et al., 2012; Morrissey et al., 2014), we examined 50 mitochondria within the basal, invasive side of the AC, and found 31 were within 80 nm of ER. Of these seven mitochondria were in possible contact with the ER (see Methods). These results are consistent with the possibility of MERCS formation in the AC. The average distance between AC mitochondria and ER in the 31 cases was ~44 nm (Figure 1B). However, the distance between mitochondria and ER at the site of known MERCS formation was determined in mammalian cells (Giamogante et al., 2020; Larrañaga-SanMiguel et al., 2025). As the dimensions and arrangement of mitochondria within mammalian cells can differ from *C. elegans'* mitochondria (Mondal et al., 2021; Riboul et al., 2024), it is possible that the distances are distinct in *C. elegans*. Mitochondria-ER contact sites are maintained and regulated by many protein interactions, some of which are thought to function as physical tethers, whereas others have roles in mediating calcium and lipid transport between the juxtaposed organelles (Figure 1C) (Aoyama-Ishiwatari & Hirabayashi, 2021; Ellenrieder et al., 2019). Notably, the proteins that make up these contact sites are neither exclusive nor specific to MERCS. This presents challenges in delineating specific roles for the MERCS versus functions independent of MERCS (Larrañaga-SanMiguel et al., 2025). To test the possible roles of MERCS in AC mitochondria, we compiled a list of 59 genes with either known or predicted roles in MERCS and assessed if RNAi-mediated knockdown of these genes affected high-capacity mitochondria ETC enrichment, invasive location, and morphology, as mitochondrial morphology can affect ATP output and transport (Aoyama-Ishiwatari & Hirabayashi, 2021; Carreras-Sureda et al., 2019; Chami et al., 2008; Chen et al., 2023; Diokmetzidou & Scorrano, 2025; Galmes et al., 2016; Hinton et al., 2024; Janer et al., 2016; Larsen et al., 2020; Liu et al., 2019; Moras et al., 2020; Morris et al., 2021; Paillusson et al., 2016; Puebla-Huerta et al., 2025; Toyofuku et al., 2020; Tubbs & Rieusset, 2017; Weng et al., 2017; Ziegler et al., 2021) (Figure 1D-E).

We categorized the MERCS genes screened based on the following criteria: **Calcium** – regulates or facilitates calcium signaling between the ER and mitochondria; **Morphology/Dynamics** – regulates or is directly required for mitochondrial fission or fusion; **Lipid Transport** – regulates or facilitates phospholipid or cholesterol transport between the ER and mitochondria; **Stress** – induced by or responds to mitochondrial and ER stress; **Tethering** – physically links the mitochondria and ER; **Apoptosis** – regulates or is required for ER-signaled apoptosis; **Autophagy** – regulates or is required for autophagy; and **ETC activity** – mitochondria-ER contact that is known to affect ETC activity. We found that RNAi-mediated reduction of 36 of the 59 genes reduced mitochondrial ETC enrichment, 23 perturbed mitochondrial localization, and 8 affected mitochondrial morphology. The genes that had the greatest effect on ETC enrichment, localization, and morphology were involved in calcium and/or lipid transport: of the 43 genes that affected at least one of the high-capacity mitochondria phenotypes, 25 were involved in calcium regulation and 11 in lipid transport. Interestingly, multiple genes that regulate mitochondrial fission and fusion – *drp-1*, *fis-1*, and *fzo-1*, did not appear to affect mitochondrial morphology. It is possible, however, that we did not detect more subtle morphology changes due to the limited resolution of compound microscopy. Knockdown of four genes – *tomm-40*, *pdzd-8*, *rmd-3*, and *sel-12* – affected all phenotypes examined and all four genes are involved in calcium regulation, lipid transport or both. TOMM-40 (human TOMM40) is part of the translocase complex in the outer mitochondrial membrane and has a direct role in calcium signaling from the ER, as well as an indirect role in cholesterol transport from the ER (Yang et al., 2024). PDZD-8 (human PDZD8) is an ER-resident protein that is required for calcium to be released from the ER into the mitochondria (Hirabayashi et al., 2017). RMD-3 (human RMDN3) is a mitochondrial protein that regulates calcium homeostasis, phospholipid transfer, and mitochondrial oxidative stress (De Vos et al., 2012; Ito et al., 2022; Shiiba et al., 2025). SEL-12 (human PSEN2) is an ER-resident protein that regulates calcium transport from the ER to mitochondria (Sammeta et al., 2023). The penetrant and multifaceted mitochondrial defects observed after RNAi-mediated reduction of these MERCS proteins suggests that these genes have broad regulatory roles in promoting the formation and localization of the AC's high-capacity mitochondria.

In summary, we found that AC mitochondria are in close enough proximity to form MERCS and RNAi-mediated knockdown of many MERCS encoding genes affect high-capacity mitochondrial ETC enrichment, morphology, and localization. This work lays the foundation for future studies directly examining the formation, composition and function of MERCS in the AC and deeper analysis of genes encoding MERCS components and their roles in promoting high-capacity mitochondria formation and function.

Methods

Caenorhabditis elegans were maintained at 20°C on nematode growth media (NGM) plates seeded with *Escherichia coli* strain OP50. The electron microscopy images used to measure the distance between juxtaposed mitochondrial and endoplasmic reticular membranes are from a depositary of images from previously published work (Morrissey et al., 2014). 50 mitochondria from five ACs (5-14 mitochondria from each AC) were selected based on clear edges of mitochondrial membrane. If the mitochondrial and ER membrane were clearly apparent and juxtaposed, the "straight freehand line" tool in Fiji/ImageJ was then used to measure the distance between the mitochondrion and closest ER. If the distance between mitochondrion and ER was less than 80 nm, the distance was recorded as a possible site where mitochondria-ER contact could form. Further, in cases where the mitochondria and ER were within 25 nm, it was scored as a possible direct contact given the resolution of the TEM images. If the distance was greater than 80 nm or there was no

apparent ER in the vicinity of that mitochondrion, it was not counted as a site where mitochondria-ER contact could form. The MERCS screen was performed using RNAi clones from either the Vidal or Ahringer feeding RNAi libraries, which were streaked onto LB plates containing tetracycline and ampicillin. For the MERCS screen, RNAi clones from the Ahringer feeding library were used for the following genes: *atad-3*, *C16C8.18*, *ced-9*, *F36G3.3*, *fis-1*, *fzo-1*, *itr-1*, *mcu-1*, *rmd-2*, *tspo-1*, *unc-68*, *emc-1*, *hrdl-1*, *T08G11.1*. The Vidal feeding library was used for the others. For RNAi screening, a single colony was inoculated in liquid LB plus 100 μL/mL ampicillin, then placed in a 37°C shaker for growth overnight. The double-stranded RNA (dsRNA) was induced by adding 1 μL/mL IPTG followed by shaking for an additional hour before plating onto NGM plates with IPTG and ampicillin. Screening was performed using *C. elegans* strain NK2657, which have the ETC protein NUO-1 endogenously tagged with mNeonGreen (mNG) fluorescent protein and AC-specific expression of the moesin actin-binding domain (ABD) fused to mCherry. The AC-specific mCherry was used to confirm the identity of the AC. Animals were synchronized using a standard hypochlorite synchronization protocol (Porta-de-la-Riva et al., 2012), plated at L1 larval stage , and grown for 36-40 hours until the P6.p vulval precursor cell (VPC) beneath the AC had undergone one division (referred to as the P6.p 2-cell stage). P6.p 2-cell stage animals were mounted on 5% agar pads with 1% sodium azide to anesthetize the worms and imaged on a Zeiss upright compound microscope equipped with 488 and 561 nm filters and a Nomarski prism for differential interference contrast (DIC). A total of 15 animals were scored by eye for each gene targeted by RNAi to determine if the RNAi treatment resulted in altered ETC enrichment, morphology, and/or localization. In brief, animals were scored by eye using the following criteria: (1) if the AC was not immediately apparent compared to neighboring uterine cells based on the NUO-1::mNG enrichment, then it was scored as having abnormal ETC enrichment; (2) If greater than 50% of the mitochondria were not basally localized, it was scored as abnormal localization, (3) If the greater than 25% of the mitochondria appeared excessively punctate, it was scored as having abnormal morphology. For statistical analysis GraphPad Prism was used to conduct a two-sided Fisher's exact test to determine significance compared to the empty vector control. The schematics were drawn, and the figure was assembled in Adobe Illustrator.

Reagents

Reagent	Genotype/Description	Available From
C. elegans strain NK2657 (Kenny-Ganzert et al., 2025)	*nuo-1(qy143[nuo-1::mNG]) II; qyIs50 [cdh-3p:moeABD::mCherry]*	CGC or by contacting david.sherwood@duke.edu
Vidal RNAi library (Rual et al., 2004)	Feeding RNAi library	Horizons Discovery
Ahringer RNAi library (Kamath et al., 2003)	Feeding RNAi library	DNAFORM
E. coli strain OP50	Standard food	CGC

References

Aoyama Ishiwatari S, Hirabayashi Y. 2021. Endoplasmic Reticulum–Mitochondria Contact Sites—Emerging Intracellular Signaling Hubs. Frontiers in Cell and Developmental Biology. Volume 9 - 2021 1527. DOI: 10.3389/fcell.2021.653828

Bernhard W, Rouiller C. 1956. Close topographical relationship between mitochondria and ergastoplasm of liver cells in a definite phase of cellular activity. J Biophys Biochem Cytol. 2: 73-8. 1573. PubMed ID: 13357525

Carreras Sureda A, Jana F, Urra H, Durand S, Mortenson DE, Sagredo A, et al., Hetz C. 2019. Non-canonical function of IRE1α determines mitochondria-associated endoplasmic reticulum composition to control calcium transfer and bioenergetics. Nat Cell Biol. 21: 755-767. 1554. PubMed ID: 31110288

Chami M, Oules B, Szabadkai G, Tacine R, Rizzuto R, Paterlini Brechot P. 2008. Role of SERCA1 truncated isoform in the proapoptotic calcium transfer from ER to mitochondria during ER stress. Mol Cell. 32: 641-51. 1561. PubMed ID: 19061639

Chen W, Zhao H, Li Y. 2023. Mitochondrial dynamics in health and disease: mechanisms and potential targets. Signal Transduction and Targeted Therapy. 8: 333. 1384. DOI: 10.1038/s41392-023-01547-9

De Vos KJ, Morotz GM, Stoica R, Tudor EL, Lau KF, Ackerley S, et al., Miller CC. 2012. VAPB interacts with the mitochondrial protein PTPIP51 to regulate calcium homeostasis. Hum Mol Genet. 21: 1299-311. 1539. PubMed ID: 22131369

Diokmetzidou A, Scorrano L. 2025. Mitochondria–membranous organelle contacts at a glance. Journal of Cell Science. 138 1552. DOI: 10.1242/jcs.263895

Ellenrieder L, Dieterle MP, Doan KN, Martensson CU, Floerchinger A, Campo ML, Pfanner N, Becker T. 2019. Dual Role of Mitochondrial Porin in Metabolite Transport across the Outer Membrane and Protein Transfer to the Inner Membrane. Mol Cell. 73: 1056-1065.e7. 1529. PubMed ID: 30738704

Flis VV, Daum G. 2013. Lipid transport between the endoplasmic reticulum and mitochondria. Cold Spring Harb Perspect Biol. 5 1278. PubMed ID: 23732475

Galmes R, Houcine A, Van Vliet AR, Agostinis P, Jackson CL, Giordano F. 2016. ORP5/ORP8 localize to endoplasmic reticulum-mitochondria contacts and are involved in mitochondrial function. EMBO Rep. 17: 800-10. 1556. PubMed ID: 27113756

Garde A, Kenny IW, Kelley LC, Chi Q, Mutlu AS, Wang MC, Sherwood DR. 2022. Localized glucose import, glycolytic processing, and mitochondria generate a focused ATP burst to power basement-membrane invasion. Dev Cell. 57: 732-749 e7. 22. PubMed ID: 35316617

Garde A, Sherwood DR. 2021. Fueling Cell Invasion through Extracellular Matrix. Trends in Cell Biology. 31: 445-456. 590. DOI: 10.1016/j.tcb.2021.01.006

Giacomello M, Pellegrini L. 2016. The coming of age of the mitochondria–ER contact: a matter of thickness. Cell Death & Differentiation. 23: 1417-1427. 1526. DOI: 10.1038/cdd.2016.52

Giamogante F, Barazzuol L, Brini M, Cali T. 2020. ER–Mitochondria Contact Sites Reporters: Strengths and Weaknesses of the Available Approaches. International Journal of Molecular Sciences. 21: 8157. 1572. PubMed ID: 27341186

Gomez Suaga P, Perez Nievas BG, Glennon EB, Lau DHW, Paillusson S, Morotz GM, et al., Miller CCJ. 2019. The VAPB-PTPIP51 endoplasmic reticulum-mitochondria tethering proteins are present in neuronal synapses and regulate synaptic activity. Acta neuropathologica communications. 7: 35. 545. DOI: 10.1186/s40478-019-0688-4

Hall DH, Hartwieg E, Nguyen KCQ. 2012. Chapter 4 - Modern Electron Microscopy Methods for C. elegans. Methods in Cell Biology. 107: 93-149. 1567. DOI: https://doi.org/10.1016/B978-0-12-394620-1.00004-7

Hinton A, Katti P, Mungai M, Hall DD, Koval O, Shao J, et al., Abel ED. 2024. ATF4-dependent increase in mitochondrial-endoplasmic reticulum tethering following OPA1 deletion in skeletal muscle. J Cell Physiol. 239: e31204. 1549. PubMed ID: 38419397

Hirabayashi Y, Kwon SK, Paek H, Pernice WM, Paul MA, Lee J, et al., Polleux F. 2017. ER-mitochondria tethering by PDZD8 regulates Ca(2+) dynamics in mammalian neurons. Science. 358: 623-630. 1536. PubMed ID: 29097544

Ito N, Takahashi T, Shiiba I, Nagashima S, Inatome R, Yanagi S. 2022. MITOL regulates phosphatidic acid-binding activity of RMDN3/PTPIP51. J Biochem. 171: 529-541. 1537. PubMed ID: 34964862

Janer A, Prudent J, Paupe V, Fahiminiya S, Majewski J, Sgarioto N, et al., Shoubridge EA. 2016. SLC25A46 is required for mitochondrial lipid homeostasis and cristae maintenance and is responsible for Leigh syndrome. EMBO Mol Med. 8: 1019-38. 1563. PubMed ID: 27390132

Kamath RS, Fraser AG, Dong Y, Poulin G, Durbin R, Gotta M, et al., Ahringer J. 2003. Systematic functional analysis of the Caenorhabditis elegans genome using RNAi. Nature. 421: 231-237. 135. DOI: 10.1038/nature01278

Kenny Ganzert IW, Basta LP, Wang L, Chi Q, Su C, Morton KS, Meyer JN, Sherwood DR. 2025. Specialized high-capacity mitochondria fuel cell invasion. bioRxiv: 2025.05.02.651978. 1525. DOI: 10.1101/2025.05.02.651978

Kenny Ganzert IW, Sherwood DR. 2024. The C. elegans anchor cell: A model to elucidate mechanisms underlying invasion through basement membrane. Semin Cell Dev Biol. 154: 23-34. 1303. PubMed ID: 37422376

Larranaga San Miguel A, Bengoa Vergniory N, Flores Romero H. 2025. Crosstalk between mitochondria-ER contact sites and the apoptotic machinery as a novel health meter. Trends Cell Biol. 35: 33-45. 1545. PubMed ID: 39379268

Larsen MC, Lee J, Jorgensen JS, Jefcoate CR. 2020. STARD1 Functions in Mitochondrial Cholesterol Metabolism and Nascent HDL Formation. Gene Expression and Molecular mRNA Imaging Show Novel Splicing and a 1:1 Mitochondrial Association. Front Endocrinol (Lausanne). 11: 559674. 1564. PubMed ID: 33193082

Lewis SC, Uchiyama LF, Nunnari J. 2016. ER-mitochondria contacts couple mtDNA synthesis with mitochondrial division in human cells. Science. 353: aaf5549. 1514. DOI: doi:10.1126/science.aaf5549

Li Y, Yao L, Mori Y, Sun SX. 2019. On the energy efficiency of cell migration in diverse physical environments. Proc Natl Acad Sci U S A. 116: 23894-23900. 1458. PubMed ID: 31719206

Liu Y, Ma X, Fujioka H, Liu J, Chen S, Zhu X. 2019. DJ-1 regulates the integrity and function of ER-mitochondria association through interaction with IP3R3-Grp75-VDAC1. Proc Natl Acad Sci U S A. 116: 25322-25328. 1559. PubMed ID: 31767755

Loncke J, Kaasik A, Bezprozvanny I, Parys JB, Kerkhofs M, Bultynck G. 2021. Balancing ER-Mitochondrial Ca(2+) Fluxes in Health and Disease. Trends Cell Biol. 31: 598-612. 1547. PubMed ID: 33678551

Marshansky V, Futai M. 2008. The V-type H+-ATPase in vesicular trafficking: targeting, regulation and function. Curr Opin Cell Biol. 20: 415-26. 1454. PubMed ID: 18511251

Mondal S, Dubey J, Awasthi A, Sure GR, Vasudevan A, Koushika SP. 2021. Tracking Mitochondrial Density and Positioning along a Growing Neuronal Process in Individual C. elegans Neuron Using a Long-Term Growth and Imaging Microfluidic Device. eNeuro. 8 1574. PubMed ID: 34035072

Moras M, Hattab C, Gonzalez Menendez P, Martino S, Larghero J, Le Van Kim C, et al., Ostuni MA. 2020. Downregulation of Mitochondrial TSPO Inhibits Mitophagy and Reduces Enucleation during Human Terminal Erythropoiesis. Int J Mol Sci. 21 1566. PubMed ID: 33260618

Morris JL, Gillet G, Prudent J, Popgeorgiev N. 2021. Bcl-2 Family of Proteins in the Control of Mitochondrial Calcium Signalling: An Old Chap with New Roles. Int J Mol Sci. 22 1551. PubMed ID: 33918511

Morrissey MA, Keeley DP, Hagedorn EJ, Mc Clatchey STH, Chi Q, Hall DH, Sherwood DR. 2014. B-LINK: a hemicentin, plakin, and integrin-dependent adhesion system that links tissues by connecting adjacent basement membranes. Developmental Cell. 31: 319-331. 31. DOI: 10.1016/j.devcel.2014.08.024

Nakamura K, Aoyama Ishiwatari S, Nagao T, Paaran M, Obara CJ, Sakurai Saito Y, et al., Hirabayashi Y. 2025. Mitochondrial complexity is regulated at ER-mitochondria contact sites via PDZD8-FKBP8 tethering. Nat Commun. 16: 3401. 1546. PubMed ID: 40246839

Namba T. 2019. BAP31 regulates mitochondrial function via interaction with Tom40 within ER-mitochondria contact sites. Science Advances. 5: eaaw1386. 547. DOI: 10.1126/sciadv.aaw1386

Paillusson S, Stoica R, Gomez Suaga P, Lau D, Mueller S, Miller T, Miller C. 2016. There's Something Wrong with my MAM; the ER–Mitochondria Axis and Neurodegenerative Diseases. Trends in Neurosciences. 39 1565. DOI: 10.1016/j.tins.2016.01.008

Park K, Garde A, Thendral SB, Soh AWJ, Chi Q, Sherwood DR. 2024. De novo lipid synthesis and polarized prenylation drive cell invasion through basement membrane. Journal of Cell Biology. 223 1400. DOI: 10.1083/jcb.202402035

Porta De La Riva M, Fontrodona L, Villanueva A, Ceron J. 2012. Basic Caenorhabditis elegans methods: synchronization and observation. Journal of Visualized Experiments: e4019. 535. DOI: 10.3791/4019

Puebla Huerta A, Huerta H, Quezada Gutierez C, Morgado Caceres P, Casanova Canelo C, Nino SA, et al., Cardenas JC. 2025. Calcium (Ca2+) fluxes at mitochondria-ER contact sites (MERCS) are a new target of senolysis in therapy-induced senescence (TIS). npj Aging. 11: 11. 1560. DOI: 10.1038/s41514-025-00197-1

Riboul DV, Crill S, Oliva CD, Restifo MG, Joseph R, Joseph K, et al., Macleod GT. 2024. Ultrastructural analysis reveals mitochondrial placement independent of synapse placement in fine caliber C. elegans neurons. bioRxiv 1575. PubMed ID: 37398149

Rual JF, Ceron J, Koreth J, Hao T, Nicot AS, Hirozane Kishikawa T, et al., Vidal M. 2004. Toward improving Caenorhabditis elegans phenome mapping with an ORFeome-based RNAi library. Genome Research. 14: 2162-2168. 194. DOI: 10.1101/gr.2505604

Sammeta SS, Banarase TA, Rahangdale SR, Wankhede NL, Aglawe MM, Taksande BG, et al., Kale MB. 2023. Molecular understanding of ER-MT communication dysfunction during neurodegeneration. Mitochondrion. 72: 59-71. 1540. DOI: https://doi.org/10.1016/j.mito.2023.07.005

Sassano ML, Felipe Abrio B, Agostinis P. 2022. ER-mitochondria contact sites; a multifaceted factory for Ca(2+) signaling and lipid transport. Front Cell Dev Biol. 10: 988014. 1544. PubMed ID: 36158205

Shah N, Colbert KN, Enos MD, Herschlag D, Weis WI. 2015. Three αSNAP and 10 ATP molecules are used in SNARE complex disassembly by N-ethylmaleimide-sensitive factor (NSF). J Biol Chem. 290: 2175-88. 1459. PubMed ID: 25492864

Shiiba I, Ito N, Oshio H, Ishikawa Y, Nagao T, Shimura H, et al., Yanagi S. 2025. ER-mitochondria contacts mediate lipid radical transfer via RMDN3/PTPIP51 phosphorylation to reduce mitochondrial oxidative stress. Nature Communications. 16: 1508. 1538. DOI: 10.1038/s41467-025-56666-4

microPublication
BIOLOGY
μP

Toyofuku T, Okamoto Y, Ishikawa T, Sasawatari S, Kumanogoh A. 2020. LRRK 2 regulates endoplasmic reticulum–mitochondrial tethering through the PERK -mediated ubiquitination pathway. The EMBO Journal. 39 1555. DOI: 10.15252/embj.2020105826

Tubbs E, Rieusset J. 2017. Metabolic signaling functions of ER-mitochondria contact sites: role in metabolic diseases. J Mol Endocrinol. 58: R87-r106. 1558. PubMed ID: 27965371

Weng TY, Tsai SA, Su TP. 2017. Roles of sigma-1 receptors on mitochondrial functions relevant to neurodegenerative diseases. J Biomed Sci. 24: 74. 1562. PubMed ID: 28917260

Yang NV, Chao JY, Garton KA, Tran T, King SM, Orr J, et al., Krauss RM. 2024. TOMM40 regulates hepatocellular and plasma lipid metabolism via an LXR-dependent pathway. Mol Metab. 90: 102056. 1535. PubMed ID: 39489289

Ziegler DV, Martin N, Bernard D. 2021. Cellular senescence links mitochondria-ER contacts and aging. Communications Biology. 4: 1323. 1550. DOI: 10.1038/s42003-021-02840-5

Citation: Kenny-Ganzert IW, Sherwood DR. 2025. Mitochondria-ER contact site components regulate the formation and localization of specialized high-capacity mitochondria in the *C. elegans* anchor cell.. microPublication Biology. 10.17912/micropub.biology.001679